Thailand Statistician
July 2026; 24(3): 668-690
http://statassoc.or.th
Contributed paper

Designing an Efficient Exponentially Weighted Moving Average Control Chart to Monitor the Mean of a Time-Series Process

Wilasinee Peerajit*
Department of Applied Statistics, Faculty of Applied Science, King Mongkut's University of Technology North Bangkok, Bangkok, Thailand.
*Corresponding author; e-mail: wilasinee.p@sci.kmutnb.ac.th

Received: 11 November 2025
Revised: 31 January 2026
Accepted: 23 February 2026

Abstract

This study covers the design of an efficient exponentially weighted moving average (EWMA) control chart for monitoring the mean of a time-series process characterized by long-memory dependence. Specifically, the study is focused on a fractionally integrated seasonal moving average process with an exogenous variable and exponential white noise. The structure of the proposed EWMA control chart is first formulated, followed by an evaluation of its performance based on the average run length (ARL) via a simulation study. An analytical expression for the ARL is derived through explicit formulas obtained by solving integral equations, while an approximated ARL is computed via a numerical integral equation approach. The existence and uniqueness of the analytical ARL solution are theoretically guaranteed using Banach's fixed-point theorem. The simulation results reveal that both the analytical and approximated ARL methods produce comparable out-of-control ARL values, with similar accuracy. The simulation results reveal that both the analytical and approximate ARL methods produced comparable out-of-control ARL values, exhibiting similar accuracy in terms of detection performance. Nevertheless, the analytical approach based on explicit formulas demonstrated a clear computational advantage: achieving faster processing times while maintaining accuracy, as evidenced by a significantly lower average time-to-signal (ATS) criterion. These findings indicate that the explicit formula performs effectively for detecting shifts in process mean values. Therefore, this approach is recommended for practical applications. An illustrative example using real-world data further confirms the effectiveness and applicability of the proposed analytical ARL method in time-series process monitoring.

Keywords: Average run length (ARL), integral equation, exponential white noise, long-memory fractionally integrated SMAX, exogenous variable.

1. Introduction

In modern production processes, manufacturers aim to deliver high-quality products with minimal defects and variation in product attributes. Statistical process control (SPC) is widely employed to monitor, control, and improve production processes using control charts. Shewhart (1931) introduced the first control chart under the assumption that the observations follow a normal distribution and are

independent and identically distributed with a constant mean and variance. However, real-world data often violate these assumptions. To overcome these limitations, Page (1954) proposed the cumulative sum (CUSUM) control chart, which accumulates information from sequential observations to detect small shifts more effectively. Roberts (1959) later developed the exponentially weighted moving average (EWMA) control chart, which is particularly sensitive to small shifts in the process mean and has been extensively applied in quality control studies. The focus of the present study is on the EWMA control chart due to its efficiency in detecting gradual process changes and its suitability for upper-sided monitoring applications.

In general, traditional control charts have been developed under the assumption that the observations generated by a process are independent and normally distributed. However, this assumption is often violated in practice because real-world data frequently exhibit autocorrelation and other time-dependent behaviors. The performance of control charts can be significantly affected by autocorrelation among successive observations. Studies by Johnson and Bagshaw (1974) and Bagshaw and Johnson (1975) demonstrate that even small autocorrelations in autocorrelated (AR) order 1 AR(1) or moving average (MA) order 1 MA(1) processes can delay the detection of out-of-control (OOC) signals in conventional control charts. Consequently, many researchers have explored the performance of control charts for AR processes such as $\text{ARMA}(p,q)$ (Yashchin 1993, Böhm and Hackl 1996, Lu and Reynolds 2001, Chang and Wu 2011, Atienza et al. 2002).

Real-world processes often exhibit trend, seasonality, and autocorrelation, characteristics effectively modeled by time-series frameworks such as AR, MA, and Autoregressive Integrated Moving Average (ARIMA) models. Therein, residuals or white noise ideally represent random fluctuations. While Gaussian white noise is the most common assumption, some processes exhibit non-Gaussian behavior, such as exponentially distributed white noise, when investigating physical and environmental phenomena such as wind speed, water flow, and oxygen concentration. (Jacob and Lewis 1977, Mohamed and Hocine 2003, Pereira and Turkman 2004, Suparman 2018).

Although traditional ARIMA models can capture short-memory dynamics, many real-world datasets display long-memory or fractional dependence, where correlations persist across long time intervals. To address this limitation, Granger and Joyeux (1980) introduced the AR fractionally integrated MA (ARFIMA) model, which allows the differencing parameter *d* to take fractional values, thereby capturing the slow decay of autocorrelation. Further extending this framework, Hosking (1981) and Barbara (2006) incorporated seasonal differencing parameter D to provide the seasonal ARFIMA (SARFIMA) model, which combines long-memory and periodic structures. The $\text{SARFIMA}(P,D,Q)_s$ process exhibits long-memory behavior when $D < 0.5,$ short-memory behavior when $D = 0,$ and intermediate-memory behavior when $D < 0.$ Several estimation methods, such as Whittle, semi-parametric, and conditional sum-of-squares approaches, have been developed to fit SARFIMA models effectively (Ndongo et al. 2010, Mostafaei and Sakhabakhsh 2012, Reisen et al. 2014). These methods have demonstrated SARFIMA's superior capability in modeling long-memory and seasonal behaviors in complex data, including applications in energy, finance, and environmental studies.

In some cases, time-series data are influenced by external or exogenous variables, such as inflation or exchange rates. Incorporating them improves accuracy and forecasting performance, resulting in the $\text{ARFIMAX}(p,d,q,r)$ model, where r represents the exogenous variable (Degiannakis 2008). Ebens (1999) proposed a simplified version without the AR term, known as the $\text{FIMAX}(d,q,r)$ model. According to Charles et al. (2001), the MA structure is particularly useful for forecasting because it smooths random variations and emphasizes underlying trends and cycles.

Consequently, the FIMAX model with an incorporated seasonal component is the FISMAX model; the version with exponential white noise is of particular interest because of its effectiveness in modeling real-world economic indicators and quality control data.

Control chart design for time-dependent processes extends the classical SPC framework by integrating time-series structures into chart statistics (Nikiforov 1975, Yashchin 1993, Knoth and Frisén 2012). This has motivated the adaptation of various control charts (including Shewhart, CUSUM, and EWMA) for autocorrelated or long-memory processes such as ARIMA and ARFIMA. For instance, Rabyk and Schmid (2016) developed the EWMA control chart specifically for detecting mean shifts in long-memory processes, which demonstrated improved sensitivity compared to traditional control charts. Similarly, Pan and Chen (2008) showed that residual control charts based on ARFIMA models were more effective than ARIMA-based ones for monitoring Taiwan's air quality. Ramjee (2000) found that the standard Shewhart and EWMA control charts performed poorly with correlated observations for ARFIMA models, leading to the development of the Hyperbolic Weighted Moving Average (HWMA) control chart. Later, Ramjee et al. (2002) extended this to the forecast-based HWMA control chart optimized for non-stationary ARFIMA processes.

Assessing the performance of the EWMA control chart can be accomplished by using a key performance metric, the average run length (ARL), which indicates the expected number of observations until an OOC signal is detected. The ARL is typically categorized into in-control (IC) (ARL_0) and OOC (ARL_1) components. Methods for evaluating the ARL include Monte Carlo simulations, Markov Chain approaches, and the integral equation, which allows for both analytical (explicit formulas) and numerical integral equation (NIE) method (Hawkins and Olwell 1998, Champ and Rigdon 1991, Areepong and Sukparungsee 2010). Previous studies have demonstrated that analytical ARL approaches are highly accurate with reduced computational times compared to simulation-based approaches (Piyaphon et al. 2014, Peerajit 2022, Peerajit 2023).

Given its ability to incorporate both sampling and processing times, the average time to signal (ATS) criterion provides a more comprehensive measure of control chart performance, particularly in multi-stage or time-dependent processes (Zou et al. 2008). Therefore, in the present study, the ATS was employed to evaluate the monitoring efficiency of the EWMA control chart. The latter (known for its strong sensitivity to small and moderate process mean shifts) combined with the ATS measure offers an effective framework for detecting changes in the process mean. ATS is also a widely used performance measure in both industrial applications and academic research (He and Grigoryan 2005, Shamsuzzaman et al. 2005, Zhang and Wu 2006). Despite these advancements, ARL evaluation for long-memory time-series processes on the EWMA control chart, particularly for FISMAX models with exponential white noise, remains scarce. Therefore, the aims of the study are to (1) derive an explicit formula for the ARL of FISMAX processes with long-memory observations and exponential white noise on the EWMA control chart, (2) approximate the ARL using the NIE method with the composite midpoint rule, and (3) compare the explicit formula and the NIE method in terms of ARL and ATS results.

The remainder of the article is organized as follows. In Section 2, the structure of the upper-sided EWMA control chart for a FISMAX model with exponential white noise is briefly described. Section 3 presents the solution for the integral equations for the ARL using the explicit formula for the proposed EWMA control chart. Section 5 provides a comparison of the ARL methods and ATS for evaluating the performance of the control chart. Section 6 presents an application of the proposed method to real data. Finally, Section 7 offers conclusions based on the results of the study.

2. A Brief Review of Control Charts

2.1. The one-sided EWMA control chart

The EWMA control chart, a memory-type control chart, was initially presented by Montgomery (2009) and discussed in detail by Roberts (1959). It is designed to detect small shifts in the process mean. The EWMA statistic is computed as the weighted average of the current and all previous subgroup means, where the weights decrease exponentially for older observations. The weight of past data is controlled by applying a smoothing parameter (λ) and can be expressed using the following recursive formula

$$e_t = \lambda y_t + (1-\lambda)e_{t-1}, \text{ for } t \geq 1, \tag{1}$$

where e_{t-1} is the EWMA statistic from the previous period (initially $e_0 = \varphi$), and y_t represents a fractionally integrated SMAX model with exponential white noise on the upper-sided EWMA control chart.

The mean of the statistic is $E(e_t) = \mu_0$ and the variance is $V(e_t)$ with the limiting value of $V(e_t) = \sigma^2\left(\frac{\lambda}{2-\lambda}\right)\left[1-(1-\lambda)^{2t}\right]$, where σ is the process standard deviation. As t approaches infinity, the term $(1-\lambda)^{2t}$ approaches zero. Thus, the variance of the statistic becomes $V(e_t) = \sigma^2\left(\frac{\lambda}{2-\lambda}\right)$. The target value, which typically corresponds to the process mean (μ), is represented by the center line (CL) of the EWMA control chart statistic. The upper control limit (UCL) and lower control limit (LCL) of the EWMA statistic can be expressed as

$$(\text{UCL, LCL}) = \mu_0 \pm L\sigma\sqrt{\frac{\lambda}{2-\lambda}}, \tag{2}$$

where L represents the width of the control limits, $0 < \lambda \leq 1$: the smaller the value of λ, the more sensitive the control chart becomes. Specifically, when $\lambda = 1$, the EWMA control chart reduces to a Shewhart control chart (i.e., becomes memoryless).

The process is considered as IC when $0 < e_t < H$ and OOC when $e_t > H$; H represents the pre-established UCL for the control chart. Accordingly, the stopping time for detecting a shift when the process exceeds the upper-sided EWMA control chart limit is given by

$$\tau_H = \inf\{t \geq 0;\, e_t > H\}, \text{ for } \varphi < H, \tag{3}$$

2.2. The FISMAX time series

Let y_t be a FISMAX process of order (D,Q,r). The resulting FISMAX$(D,Q,r)_S$ model with exponential white noise can be written as

$$(1-B^s)^D y_t = \Theta_0 + \Theta_s(B)\varepsilon_t + \sum_{j=1}^{r}\varpi_j x_{jt}, \tag{4}$$

where Θ_0 is a constant (intercept) term; x_{jt}, $j = 1,2,...,r$ are the exogenous variables; t is the time; and ϖ_j are the corresponding coefficient variables. $\Theta_s(B) = 1-\Theta_1 B^s - \Theta_2 B^{s2} - ... - \Theta_Q B^{sQ}$ is the seasonal MA polynomial of order Q with coefficients $\Theta_i, i = 1,2,...,Q$. The seasonal fractional differencing (or integration) operator $(1-B^s)^D$ can be expanded using the binomial series (Hosking, 1981) as follows:

$$(1-B^s)^D = \sum_{r=0}^{\infty} \binom{D}{r} (-1)^r B^{sr},$$

which can be expressed more explicitly as

$$(1-B^s)^D = 1 - DB^s + \frac{D(D-1)}{2!} B^{2s} - \frac{D(D-1)(D-2)}{6} B^{3s} + \ldots, \quad (5)$$

where B is the backshift operator; $B^Q y_t = y_{t-Q}$; s denotes the seasonal period (e.g. $s = 12$ for monthly data with annual seasonality); non-integer D is the seasonal fractional differencing or long-memory parameter ($0 < D < 0.5$), and ε_t denotes the exponential white noise ($\varepsilon_t \sim Exp(\beta)$).

Simplifying (4) and (5) yields a generalized FISMAX model as follows:

$$y_t = \Theta_0 + \varepsilon_t - \sum_{i=1}^{Q} \Theta_i \varepsilon_{t-Si} + \sum_{j=1}^{r} \varpi_j x_{jt} + D y_{t-s} - \frac{D(D-1)}{2!} y_{t-2s} + \frac{D(D-1)(D-2)}{6} y_{t-3s} - \ldots, \quad (6)$$

where $\varepsilon_t \sim Exp(\beta)$, and $E(\varepsilon_t) = \beta$ represents the mean. It is important to note that the process mean equals 1 when the process is IC ($\beta = \beta_0$), whereas it becomes $\beta = \beta_1$, when the process is OOC. The process mean can therefore be expressed as

$$\beta_1 = \beta_0 (1 + \delta),$$

where δ represents the magnitude of the shift in the process mean. In the present study, the focus is exclusively on long-memory processes, so the model parameters were aligned to ensure consistency with the research objectives.

3. Development of Explicit Formulas for the ARL of the EWMA Control Chart with a FISMAX Process

Here, the analytical ARL is derived using integral equations via the explicit formula method for detecting shifts in the process mean of the FISMAX$(D,Q,r)_S$ model with exponential white noise. Furthermore, the existence and uniqueness of the analytical ARL solution are demonstrated using Banach's fixed-point theorem.

In preliminary ARL computations, the EWMA control chart responsive to both upper- and lower-sided process mean shifts is considered. Here, the present formulation focuses exclusively on upper-sided process mean shifts by adopting the CL at LCL = 0 and defining the UCL as $H > 0$.

Let $\mathcal{L}(\varphi)$ denote the analytical ARL associated with detecting changes in the mean of a long-memory FISMAX$(D,Q,r)_S$ process with exponential white noise under the EWMA control scheme, where $E_0 = \varphi$ is the initial value of the monitoring statistic. Consequently, a unique solution for the ARL using integral equations for $\mathcal{L}(\varphi) = E_\infty(\tau_H) < \infty,$ is defined as

$$\mathcal{L}(\varphi) = \left\{1 - P\left(\frac{(1-\lambda)\varphi - \lambda\mathcal{K}}{\lambda} < \varepsilon_1 < \frac{H - (1-\lambda)\varphi - \lambda\mathcal{K}}{\lambda}\right)\right\} + \int_{\frac{-(1-\lambda)\varphi - \lambda\mathcal{K}}{\lambda}}^{\frac{H-(1-\lambda)\varphi-\lambda\mathcal{K}}{\lambda}} \left(1 + \mathcal{L}((1-\lambda)\varphi + \lambda(\mathcal{K}))\, f(\varepsilon) d\varepsilon\right.$$

$$\mathcal{L}(\varphi) = 1 + \int_{\frac{-(1-\lambda)\varphi - \lambda\mathcal{K}}{\lambda}}^{\frac{H-(1-\lambda)\varphi-\pi\mathcal{K}}{\lambda}} \mathcal{L}((1-\lambda)\varphi + \lambda(\mathcal{K}))\, f(\varepsilon) d\varepsilon,$$

where $\mathcal{K} = \Theta_0 - \sum_{i=1}^{Q} \Theta_i \varepsilon_{t-Si} + \sum_{j=1}^{r} \varpi_j x_{jt} + D y_{t-s} - \frac{D(D-1)}{2!} y_{t-2s} + \frac{D(D-1)(D-2)}{6} y_{t-3s} - \ldots,$

By modifying the integral variable, we can derive the integral equations as

$$\mathcal{L}(\varphi) = 1 + \frac{1}{\lambda}\int_0^H \mathcal{L}(g)\, f\left(\frac{g-(1-\lambda)\varphi}{\lambda} - \mathcal{K}\right) dg. \tag{7}$$

From the above considerations, the integral equations for the analytical ARL can be expressed as

$$\mathcal{L}(\varphi) = 1 + \frac{1}{\lambda\beta}\int_0^H \mathcal{L}(g) e^{-\frac{g}{\lambda\beta}} . e^{\left(\frac{(1-\lambda)\varphi}{\lambda\beta} + \frac{\mathcal{K}}{\lambda}\right)} dg. \tag{8}$$

Operator $\mathcal{T}$ is considered a contraction on the metric space of continuous functions $(\mathcal{C}(I), \| \|_1)$, where I is defined over a complete interval, equipped with the norm $\|\mathcal{L}\| = \underset{\varphi\in \mathrm{I}}{Sup}|\mathcal{L}(\varphi)|$. If constant $\rho \in [0, 1)$ exists such that $\|\mathcal{T}(\mathcal{L}_1) - \mathcal{T}(\mathcal{L}_2)\| \le \rho\|\mathcal{L}_1 - \mathcal{L}_2\|$ for all $\mathcal{L}_1, \mathcal{L}_2 \in [0, H]$, then $\mathcal{T}$ satisfies the contraction condition. Accordingly, the existence and uniqueness of the analytical ARL solution can be verified via Banach's fixed-point theorem.

Let $\mathcal{C}(I_1)$ represent the class of all continuous functions defined on compact interval $I_1 = [0, H]$. In (8), the right-hand side is continuous, so the integral is a continuous function. Hence, the integral equations become

$$\mathcal{T}\left(\mathcal{L}(\varphi)\right) = 1 + \frac{1}{\lambda\beta}\int_0^H \mathcal{L}(g) e^{-\frac{g}{\lambda\beta}} . e^{\left(\frac{(1-\lambda)\varphi}{\lambda\beta} + \frac{\mathcal{K}}{\beta}\right)} dg. \tag{9}$$

Consequently, the integral equations can be expressed as

$$\mathcal{T}\left(\mathcal{L}(\varphi)\right) = \mathcal{L}(\varphi).$$

Proposition 1 *Operator $\mathcal{T}$ is a contraction on metric space $M = (\mathcal{C}(I), \| \|_1)$ with the norms*

$$\|\mathcal{L}\| = \underset{\varphi\in \mathrm{I}}{Sup}|\mathcal{L}(\varphi)|.$$

Proof: $\mathcal{T}$ is a contraction based on inequality $\|\mathcal{T}(\mathcal{L}_1) - \mathcal{T}(\mathcal{L}_2)\| \le \rho\|\mathcal{L}_1 - \mathcal{L}_2\|$ being valid for two variables: $\varphi \in I$ and $\mathcal{L}_1, \mathcal{L}_2 \in \mathcal{C}(I)$, where $\rho \in [0, 1)$ is a positive constant. As per (9), we can conclude that

$$\begin{aligned}
\|\mathcal{T}(\mathcal{L}_1) - \mathcal{T}(\mathcal{L}_2)\| &= \underset{\varphi\in[0,H]}{Sup}\left|\mathcal{L}_1(g) - \mathcal{L}_2(g)\frac{1}{\lambda\beta}e^{\frac{(1-\lambda)\varphi}{\lambda\beta}+\frac{\mathcal{K}}{\beta}}\int_0^H \mathcal{T}(g)e^{-\frac{g}{\lambda\beta}}dg\right| \\
&\le \underset{\varphi\in[0,H]}{Sup}\left|\|\mathcal{L}_1 - \mathcal{L}_2\|\frac{1}{\lambda\beta}e^{\frac{(1-\lambda)\varphi}{\lambda\beta}+\frac{\mathcal{K}}{\beta}}(-\lambda\beta)(e^{-\frac{H}{\lambda\beta}} - 1)\right| \\
&= \|\mathcal{L}_1 - \mathcal{L}_2\| \underset{\varphi\in[0,H]}{Sup}\left[\frac{1}{\lambda\beta}e^{\frac{(1-\lambda)\varphi}{\lambda\beta}+\frac{\mathcal{K}}{\beta}}.(1 - e^{-\frac{H}{\lambda\beta}})\right] \\
&= \|\mathcal{L}_1 - \mathcal{L}_2\| \underset{\varphi\in[0,H]}{Sup}\left[e^{\frac{(1-\lambda)\varphi}{\lambda\beta}+\frac{\mathcal{K}}{\beta}}.(1 - e^{-\frac{H}{\lambda\beta}})\right].
\end{aligned}$$

Consequently, we can obtain

$$\|\mathcal{T}(\mathcal{L}_1) - \mathcal{T}(\mathcal{L}_2)\| \le \rho\|\mathcal{L}_1 - \mathcal{L}_2\|, \text{ where } \rho = \underset{\varphi\in[0,H]}{Sup}\left[e^{\frac{(1-\lambda)\varphi}{\lambda\beta}+\frac{\mathcal{K}}{\lambda}}.(1 - e^{-\frac{H}{\lambda\beta}})\right].$$

The triangle inequality can be applied by considering

$$\left|\mathcal{L}_1-\mathcal{L}_2\right|=\underset{\varphi\in[0,H]}{Sup}\left|\mathcal{L}_1-\mathcal{L}_2\right|=\left\|\mathcal{L}_1-\mathcal{L}_2\right\|.$$

Therefore, operator $\mathcal{T}$ is a contraction, which implies that the corresponding fixed-point equation $\mathcal{T}\left(\mathcal{L}(\varphi)\right)=\mathcal{L}(\varphi)$ possesses a unique solution, in accordance with Banach's fixed-point theorem. In the subsequent analysis, we focus on the integral equations presented in (8).

For $D(\varphi)=e^{\left(\frac{(1-\lambda)\varphi}{\lambda\beta}+\frac{\mathcal{K}}{\beta}\right)}$ and $b=\int_0^H\mathcal{L}(g)e^{-\frac{g}{\lambda\beta}}dg,$ we can obtain

$$\mathcal{L}(\varphi)=1+\frac{D(\varphi)}{\lambda\beta}b,\ 0\le\varphi\le H. \tag{10}$$

Solving for constant $b=\int_0^H\left(1+\frac{D(g)}{\lambda\beta}b\right).e^{-\frac{g}{\lambda\beta}}dg$ enables us to derive the following equations:

$$\begin{aligned} b &= \int_0^H e^{-\frac{g}{\lambda\beta}}dg+b\int_0^H\frac{D(g)}{\lambda\beta}e^{-\frac{g}{\lambda\beta}}dg = \lambda\beta(1-e^{-\frac{H}{\lambda\beta}})+\frac{b}{\lambda\beta}e^{\left(\frac{\mathcal{K}}{\beta}\right)}.\int_0^H e^{\left(\frac{(1-\lambda)\varphi}{\lambda\beta}+\frac{g}{\lambda\beta}\right)}dg \\ &= \lambda\beta(1-e^{-\frac{H}{\lambda\beta}})+\frac{b}{\lambda}e^{\left(\frac{\mathcal{K}}{\beta}\right)}.(1-e^{-\frac{H}{\beta}}) = \frac{\lambda\beta(1-e^{-\frac{H}{\lambda\beta}})}{1-\frac{1}{\lambda}e^{\left(\frac{\mathcal{K}}{\beta}\right)}.(1-e^{-\frac{H}{\beta}})}. \end{aligned}$$

By substituting constant b into (10), the function $\mathcal{L}(\varphi)$ can be expressed as

$$\begin{aligned} \mathcal{L}(\varphi) &= 1+\frac{e^{\left(\frac{(1-\lambda)\varphi}{\lambda\beta}+\frac{\mathcal{K}}{\beta}\right)}}{\pi\lambda}.\frac{\lambda\beta(1-e^{-\frac{H}{\lambda\beta}})}{1-\frac{1}{\pi}e^{\left(\frac{\mathcal{K}}{\beta}\right)}.(1-e^{-\frac{H}{\beta}})}=1+e^{\left(\frac{(1-\lambda)\varphi}{\lambda\beta}+\frac{\mathcal{K}}{\beta}\right)}.\frac{\lambda(1-e^{-\frac{H}{\lambda\beta}})}{\lambda-(1-e^{-\frac{H}{\beta}}).e^{\left(\frac{\mathcal{K}}{\beta}\right)}} \\ &= 1-\frac{e^{\left(\frac{(1-\lambda)\varphi}{\lambda\beta}+\frac{\mathcal{K}}{\beta}\right)}\lambda(e^{-\frac{H}{\lambda\beta}}-1)}{\lambda+e^{\left(\frac{\mathcal{K}}{\beta}\right)}(e^{-\frac{H}{\beta}}-1).}. \end{aligned}$$

Consequently, by solving the integral equations, the explicit formulations for the ARL are derived as follows:

$$\mathcal{L}(\varphi)=1-\frac{e^{\left(\frac{(1-\lambda)\varphi}{\lambda\beta}\right)}\lambda(e^{-\frac{H}{\lambda\beta}}-1)}{\lambda e^{\left(-\frac{\mathcal{K}}{\beta}\right)}+(e^{-\frac{H}{\beta}}-1)},$$

where $\mathcal{K}=\Theta_0-\sum_{i=1}^{Q}\Theta_i\varepsilon_{t-Si}+\sum_{j=1}^{r}\varpi_j x_{jt}+Dy_{t-s}-\frac{D(D-1)}{2!}y_{t-2s}+\frac{D(D-1)(D-2)}{6}y_{t-3s}-\ldots,$

For the IC state, when the exponential parameter satisfies $\beta=\beta_0,$ the corresponding explicit formulation of ARL_0 can be expressed as

$$ARL_0=1-\frac{e^{\left(\frac{(1-\lambda)\varphi}{\lambda\beta_0}\right)}\lambda(e^{-\frac{H}{\lambda\beta_0}}-1)}{\lambda e^{\left(-\frac{1}{\beta_0}\left(\Theta_0-\sum_{i=1}^{Q}\Theta_i\varepsilon_{t-Si}+\sum_{j=1}^{r}\varpi_j x_{jt}+Dy_{t-s}-\frac{D(D-1)}{2!}y_{t-2s}+\frac{D(D-1)(D-2)}{6}y_{t-3s}-\ldots\right)\right)}+(e^{-\frac{H}{\beta_0}}-1)}, \tag{11}$$

In contrast, for the OOC state, where the exponential parameter satisfies $\beta = \beta_1$, the corresponding explicit formulation for ARL_1 becomes

$$ARL_1 = 1 - \frac{e^{\left(\frac{(1-\lambda)\varphi}{\lambda\beta_1}\right)}\lambda(e^{-\frac{H}{\lambda\beta_1}} - 1)}{\lambda e^{\left(-\frac{1}{\beta_1}\left(\Theta_0 - \sum_{i=1}^{Q}\Theta_i\varepsilon_{t-Si} + \sum_{j=1}^{r}\varpi_j x_{jt} + Dy_{t-s} - \frac{D(D-1)}{2!}y_{t-2s} + \frac{D(D-1)(D-2)}{6}y_{t-3s} - \ldots\right)\right)} + (e^{-\frac{H}{\beta_1}} - 1)}, \quad (12)$$

The algorithmic description of the explicit formulas for the ARL of the EWMA control chart with a FISMAX$(D,Q,r)_S$ model with exponential white noise is presented as follows.

Input:

1. EWMA control chart parameters:
   - Set the smoothing parameter ($\lambda = 0.05, 0.10, 0.20$)
2. Model coefficients:
   - Set the fractional differencing parameters
   - Set the values of the model coefficients ($D = 0.12, 0.25, 0.375$)
   - Set the seasonal moving average with exogenous variables coefficients ($\Theta_1 = \pm\, 0.30, \varpi_1 = 0.10$ and $\varpi_2 = 0.30$)
   - Specify the initial values of the process ($y_{t-s}, y_{t-2s}, \ldots, = 1$)
3. In-control mean:
   - Set the in-control mean $(\beta_0 = 1)$ for the in-control ARL_0 ($\varepsilon_t \sim Exp(\beta_0)$).
4. Mean shifts:
   - Define the out-of-control mean as $(\beta_1 = \beta_0(1+\delta))$, where δ = 0.125, 0.25, 0.375, 0.5, 0.625, 0.75, 0.875, and 1.0.

These inputs are used to construct of the EWMA statistic and to compute the ARL by solving the corresponding integral equations using explicit formulas.

Output:

In-control ARL Computation

1. Solve the FISMAX model defined as (y_t) for a generalized FISMAX$(D,Q,r)_S$ process with exponential white noise.
2. Determine the values of the process coefficients $(\Theta_1, \varpi_1, \varpi_2)$ and specify the initial values $(y_{t-s}, y_{t-2s}, \ldots)$
3. Specify the parameter (β_0) for the in-control exponential white noise; that is, $(\varepsilon_t \sim Exp(\beta_0))$.
4. Compute EWMA statistic (e_t) for the FISMAX$(D,Q,r)_S$ process given in (1).
5. Determine the values of the control chart coefficients for various of λ.
6. Calculate the upper control limit (UCL), denoted by H, corresponding to the desired in-control ARL_0 using (11).
7. Execute Steps 2–6 under in-control process $(\delta = 0)$, and determine the value of (H) for each (λ, κ) combination.

Out-of-control ARL Computation

8. Compute the OOC ARL_1 for shifts in the process mean (β_1), is given in (12), where the control limit (H) is obtained from Steps 6 and 7.
9. Record the computational time required to obtain the first OOC ARL_1 signal.
10. Repeat Steps 6–9 to compute ARL_1 corresponding to each specified shift size (δ).

4. Chart Parameter Selection and Performance Measures

The performance of a control chart is typically evaluated by its ability to rapidly detect an OOC process mean shift. Here, an explicit formula is proposed to evaluate the detection speed of OOC process mean shifts under two simulation scenarios: FISMAX$(D,1,1)_{12}$ and FISMAX$(D,1,2)_{12}$ with coefficient parameters $\Theta_1 = \pm\ 0.30, \varpi_1 = 0.10$ and $\varpi_2 = 0.30$. The evaluation was conducted with a long-memory level of 0.125, 0.25, and 0.375, and a mean process shift magnitude of 0.125, 0.25, 0.375, 0.5, 0.625, 0.75, 0.875, and 1.0. For comparison purposes, the EWMA control chart was analyzed using weighting parameter $\lambda = 0.05$, 0.1, or 0.3, with the target IC ARL (ARL_0) set to 370. For the IC state, the ARL_0 value corresponding to no shift in the process mean was determined based on exponential white noise parameter $\beta_0 = 1$. The accuracy of the proposed formula-based method was validated by approximating the ARL using the NIE method with the composite midpoint rule. Moreover, the proposed approach demonstrates advantages not only in detection speed, as measured by using average time to signal (ATS), but also the computational efficiency with respect to the processing time.

4.1. Derivation of the ARL using the NIE method with the composite midpoint rule

The accuracy of the proposed formula was evaluated by comparing its performance with that of the approximated ARL using the NIE method with the composite midpoint rule (Crowder 1987). The NIE method was selected as the benchmark due to its proven accuracy in approximating the ARL (Peerajit 2025).

The NIE in (8) is employed to solve an m linear system within interval [0, H] by partitioning it into $0 \le \partial_1 \le \partial_2 \le .... \le \partial_m \le H$ and applying constant weights $w_k = H/m$ as follows:

$$\int_0^H \mathcal{L}(s) f(g) dg \approx \sum_{k=1}^{m} w_k f(\partial_k), \tag{13}$$

where $\partial_k = H/m(k-0.5)$ is a set of points and $w_k = H/m;\ k = 1,2,...,m$ is a weight defined for different midpoint rules. Thus, by solving the system of linear algebraic equations, we can obtain

$$\ell(\partial_l) \approx 1 + \frac{1}{\lambda}\sum_{k=1}^{m} w_k\, \ell(\partial_k)\, f\left(\frac{\partial_k - (1-\lambda)\partial_l}{\lambda} - \left(\Theta_0 - \sum_{i=1}^{Q}\Theta_i \varepsilon_{t-Si} + \sum_{j=1}^{r}\varpi_j x_{jt} + D y_{t-s} - \frac{D(D-1)}{2!} y_{t-2s} + \frac{D(D-1)(D-2)}{6} y_{t-3s} - ...\right)\right),\ l = 1, 2, ..., m \tag{14}$$

Function $\ell(\partial_1), \ell(\partial_2), ..., \ell(\partial_m)$ yields an approximation of the ARL in (15) when ∂_l is replaced by φ, leading to

$$\ell(\varphi) \approx 1 + \frac{1}{\lambda}\sum_{k=1}^{m} w_k \ell(\partial_k)\, f\left(\frac{\partial_k - (1-\lambda)\varphi}{\lambda} - \left(\Theta_0 - \sum_{i=1}^{Q}\Theta_i \varepsilon_{t-Si} + \sum_{j=1}^{r}\varpi_j x_{jt}\right.\right.$$

$$+Dy_{t-s}-\frac{D(D-1)}{2!}y_{t-2s}+\frac{D(D-1)(D-2)}{6}y_{t-3s}-\ldots\Big)\Big)\Big], \quad (15)$$

As reported in Tables 1-6, the proposed formula exhibited ARL values that are in close agreement with those generated using the NIE-based method in (15) across all process mean shift magnitudes and long-memory conditions, thereby validating its accuracy and practicability.

4.2. Evaluating the ARL using the explicit formula

The ARL calculations obtained from the proposed formula method were validated against those obtained using the NIE method. The proposed method demonstrated its effectiveness in detecting shifts in the process mean in the OOC state on the EWMA control chart under two simulation scenarios: FISMAX(D, 1, 1)$_{12}$ and FISMAX(D, 1, 2)$_{12}$. The corresponding results are summarized in Tables 1-6.

The optimal charting parameters described above yielded the smallest ARL at $\lambda = 0.05$, which is consistent with the findings reported by Montgomery (2009), followed by $\lambda = 0.30$ and $\lambda = 0.01$. The optimal IC ARL results were obtained with $ARL_0 = 370$. For $\lambda = 0.05$, the corresponding H value was determined using (11) (the proposed formula method), resulting in $H = 1.01948 \times 10^{-7}$. Similarly, $\lambda = 0.01$ yielded $H = 0.00438661$, and $\lambda = 0.30$ produced $H = 0.34271507$, as can be seen in Columns 4-6 in Table 1. In addition, Columns 4-6 in Tables 2-6 report the corresponding H values for each value of λ. It is evident that H increases as λ increases.

The ARL_1 values reveal a clear relationship between the magnitude of the process mean shift and the speed of detection. As the magnitude of the mean shift increased, the ARL_1 value decreased, thus indicating faster detection performance across all scenarios. This reduction is particularly significant when the process mean shift magnitude was less than 0.125, which corresponds to a small process change (Montgomery 2009). These results highlight the sensitivity and effectiveness of the EWMA control chart as evaluated through using the proposed formula method to derive the ARL, which aligns with the findings of Sunthornwat et al. (2020). For moderate mean shifts, specifically in the range of $0.125 < \delta \leq 0.25$, the ARL_1 values show only a slight decrease compared to $\delta = 0.125$, thereby suggesting a diminishing rate of improvement in detection speed. Furthermore, the ARL_1 values were similar for $\delta = 0.500$, 0.625, 0.750, 0.875 and 1.000, indicating that the proposed method maintained stable detection capability for larger process mean shifts $(0.25 \leq \delta \leq 1)$.

This stability demonstrates that the proposed method provides consistent and reliable ARL detection across different levels of process mean changes, thus confirming its robustness and suitability for practical process monitoring applications.

4.3. Measurement indices

1) Computational efficiency analysis

After validating the accuracy of the proposed formula method, an analysis of its computational efficiency was also conducted. The values in parentheses in Tables 1-6 indicating the computational times for calculating the ARL show that the proposed method only took a fraction of a second across all scenarios, whereas the NIE method required approximately 11-13 seconds. Therefore, the proposed formula method demonstrates a significant advantage in terms of computational efficiency, thus making it a favorable choice for practical applications.

Table 1. ARL_1 values using the explicit formula and NIE methods for the EWMA control chart with the FISMAX(0.125, 1, 1)$_{12}$ model and exponential white noise (ARL_0 = 370)

Coefficient parameters		δ	λ		0.05		0.10		0.30
Θ_1	ϖ_1		H		0.000000101948		0.00438661		0.34271507
0.3	0.1	0.125	ARL_{Exp}	40.661	(< 0.001)	121.144	(< 0.001)	46.154	(< 0.001)
			ARL_{NIE}	40.661	(12.937)	121.144	(12.102)	46.154	(12.021)
		0.250	ARL_{Exp}	7.586	(< 0.001)	49.420	(< 0.001)	21.428	(< 0.001)
			ARL_{NIE}	7.586	(12.564)	49.420	(11.563)	21.428	(12.152)
		0.375	ARL_{Exp}	2.502	(< 0.001)	23.812	(< 0.001)	13.097	(< 0.001)
			ARL_{NIE}	2.502	(12.652)	23.812	(12.035)	13.097	(11.756)
		0.500	ARL_{Exp}	1.435	(< 0.001)	13.091	(< 0.001)	9.148	(< 0.001)
			ARL_{NIE}	1.435	(12.103)	13.091	(11.892)	9.148	(12.351)
		0.625	ARL_{Exp}	1.151	(< 0.001)	8.021	(< 0.001)	6.934	(< 0.001)
			ARL_{NIE}	1.151	(11.953)	8.021	(12.381)	6.934	(12.046)
		0.750	ARL_{Exp}	1.061	(< 0.001)	5.382	(< 0.001)	5.555	(< 0.001)
			ARL_{NIE}	1.061	(12.036)	5.382	(12.569)	5.555	(11.596)
		0.875	ARL_{Exp}	1.028	(< 0.001)	3.899	(< 0.001)	4.634	(< 0.001)
			ARL_{NIE}	1.028	(12.186)	3.899	(12.896)	4.634	(12.201)
		1.00	ARL_{Exp}	1.014	(< 0.001)	3.011	(< 0.001)	3.985	(< 0.001)
			ARL_{NIE}	1.014	(12.998)	3.011	(11.055)	3.985	(12.022)
Coefficient parameters		δ	λ		0.05		0.10		0.30
Θ_1	ϖ_1		H		0.0000000559502		0.00238452		0.17281282
-0.3	0.1	0.125	ARL_{Exp}	38.103	(< 0.001)	112.983	(< 0.001)	31.423	(< 0.001)
			ARL_{NIE}	38.103	(11.978)	112.983	(12.035)	31.423	(11.796)
		0.250	ARL_{Exp}	6.841	(< 0.001)	43.687	(< 0.001)	14.152	(< 0.001)
			ARL_{NIE}	6.841	(12.746)	43.687	(12.465)	14.152	(12.164)
		0.375	ARL_{Exp}	2.275	(< 0.001)	20.222	(< 0.001)	8.586	(< 0.001)
			ARL_{NIE}	2.275	(13.015)	20.222	(12.597)	8.586	(12.564)
		0.500	ARL_{Exp}	1.356	(< 0.001)	10.815	(< 0.001)	6.012	(< 0.001)
			ARL_{NIE}	1.356	(12.843)	10.815	(11.975)	6.012	(12.956)
		0.625	ARL_{Exp}	1.120	(< 0.001)	6.523	(< 0.001)	4.594	(< 0.001)
			ARL_{NIE}	1.120	(12.987)	6.523	(13.154)	4.594	(12.643)
		0.750	ARL_{Exp}	1.047	(< 0.001)	4.355	(< 0.001)	3.723	(< 0.001)
			ARL_{NIE}	1.047	(12.752)	4.355	(12.562)	3.723	(12.556)
		0.875	ARL_{Exp}	1.021	(< 0.001)	3.169	(< 0.01)	3.149	(< 0.001)
			ARL_{NIE}	1.021	(11.866)	3.169	(12.895)	3.149	(12.154)
		1.000	ARL_{Exp}	1.010	(< 0.001)	2.474	(< 0.001)	2.748	(< 0.001)
			ARL_{NIE}	1.010	(12.165)	2.474	(11.975)	2.748	(12.766)

The values in parentheses are the processing times in seconds.

2) Average time to signal (ATS)

ATS (defined as the expected time for a control chart to detect a shift from IC to OOC) accounts for the processing time along with the ARL (Jin and Tsung 2009), thereby providing a time-based measure of control chart sensitivity. It is calculated as

$$\text{ATS} = \text{ARL} \times t \text{ (Sec.)}, \tag{16}$$

where ARL is the OOC ARL (ARL_1) obtained using the NIE method, and t is the time interval between successive computations. A smaller ATS value indicates faster detection of process mean shifts.

Detecting a change from the IC state to the OOC state was evaluated using the processing time and ATS values. The ATS values approached zero across all cases studied using the proposed formula

method. In contrast, the NIE method produced relatively high ATS values for small mean shifts, which gradually decreased as the magnitude of the shift increased. These results are presented in Table 7.

As shown in Figures 1 and 2 for the two FISMAX models, when the magnitude of the mean shift was 0.125, the weighting parameter $\lambda = 0.03$ produced the lowest ATS values, or values very close to those obtained with $\lambda = 0.05$. For larger mean shifts (0.25-1.00), $\lambda = 0.05$ resulted in the lowest ATS values. Therefore, $\lambda = 0.05$ was deemed to be the most appropriate value for the FISMAX processes on the EWMA control chart, as confirmed through repeated validation using the NIE method in conjunction with the proposed formula method.

Table 2. ARL_1 values using the explicit formula and NIE methods for the EWMA control chart with the FISMAX$(0.25, 1, 1)_{12}$ model and exponential white noise ($ARL_0 = 370$)

Coefficient parameters		δ	λ	0.05			0.10		0.30
Θ_1	ϖ_1		H	0.0000000847657			0.00363423		0.2757058
0.3	0.1	0.125	ARL_{Exp}	39.856	(< 0.001)	118.561	(< 0.001)	40.036	(< 0.001)
			ARL_{NIE}	39.856	(12.115)	118.561	(12.564)	40.036	(12.233)
		0.250	ARL_{Exp}	7.347	(< 0.001)	47.570	(< 0.001)	18.405	(< 0.001)
			ARL_{NIE}	7.347	(12.562)	47.570	(12.365)	18.405	(12.153)
		0.375	ARL_{Exp}	2.428	(< 0.001)	22.635	(< 0.001)	11.233	(< 0.001)
			ARL_{NIE}	2.428	(12.253)	22.635	(12.486)	11.233	(12.546)
		0.500	ARL_{Exp}	1.409	(< 0.001)	12.336	(< 0.001)	7.859	(< 0.001)
			ARL_{NIE}	1.409	(12.462)	12.336	(12.766)	7.859	(12.446)
		0.625	ARL_{Exp}	1.141	(< 0.001)	7.519	(< 0.001)	5.976	(< 0.001)
			ARL_{NIE}	1.141	(13.015)	7.519	(12.663)	5.976	(12.845)
		0.750	ARL_{Exp}	1.056	(< 0.001)	5.035	(< 0.001)	4.809	(< 0.001)
			ARL_{NIE}	1.056	(12.356)	5.035	(12.651)	4.809	(12.113)
		0.875	ARL_{Exp}	1.025	(< 0.001)	3.650	(< 0.001)	4.031	(< 0.001)
			ARL_{NIE}	1.025	(11.956)	3.650	(12.064)	4.031	(12.546)
		1.000	ARL_{Exp}	1.013	(< 0.001)	2.827	(< 0.001)	3.484	(< 0.001)
			ARL_{NIE}	1.013	(12.235)	2.827	(12.355)	3.484	(12.596)
Coefficient parameters		δ	λ	0.05			0.10		0.30
Θ_1	ϖ_1		H	0.0000000465204			0.00197879		0.141400581
-0.3	0.1	0.125	ARL_{Exp}	37.350	(< 0.001)	110.603	(< 0.001)	28.769	(< 0.001)
			ARL_{NIE}	37.350	(12.335)	110.603	(12.865)	28.769	(12.496)
		0.250	ARL_{Exp}	6.629	(< 0.001)	42.077	(< 0.001)	12.850	(< 0.001)
			ARL_{NIE}	6.629	(12.986)	42.077	(12.346)	12.850	(12.667)
		0.375	ARL_{Exp}	2.213	(< 0.001)	19.244	(< 0.001)	7.775	(< 0.001)
			ARL_{NIE}	2.213	(12.456)	19.244	(12.798)	7.775	(13.048)
		0.500	ARL_{Exp}	1.335	(< 0.001)	10.210	(< 0.001)	5.445	(< 0.001)
			ARL_{NIE}	1.335	(12.796)	10.210	(13.016)	5.445	(12.975)
		0.625	ARL_{Exp}	1.112	(< 0.001)	6.133	(< 0.001)	4.169	(< 0.001)
			ARL_{NIE}	1.112	(13.016)	6.133	(11.894)	4.169	(12.466)
		0.750	ARL_{Exp}	1.044	(< 0.001)	4.093	(< 0.001)	3.389	(< 0.001)
			ARL_{NIE}	1.044	(12.645)	4.093	(12.496)	3.389	(11.798)
		0.875	ARL_{Exp}	1.019	(< 0.001)	2.985	(< 0.001)	2.877	(< 0.001)
			ARL_{NIE}	1.019	(12.765)	2.985	(12.674)	2.877	(11.995)
		1.000	ARL_{Exp}	1.009	(< 0.001)	2.341	(< 0.001)	2.521	(< 0.001)
			ARL_{NIE}	1.009	(12.896)	2.341	(12.131)	2.521	(12.466)

The values in parentheses are the processing times in seconds.

Table 3. ARL_1 values using the explicit formula and NIE methods for the EWMA control chart with the FISMAX(0.375, 1, 1)$_{12}$ model and exponential white noise ($ARL_0 = 370$)

Coefficient parameters		δ	λ		0.05		0.10		0.30
Θ_1	ϖ_1		H		0.0000000724332		0.00309754		0.23031817
0.3	0.1	0.125	ARL_{Exp}	39.183	(< 0.001)	116.413	(< 0.001)	36.187	(< 0.001)
			ARL_{NIE}	39.183	(12.556)	116.413	(12.545)	36.187	(11.944)
		0.250	ARL_{Exp}	7.150	(< 0.001)	46.056	(< 0.001)	16.501	(< 0.001)
			ARL_{NIE}	7.150	(12.688)	46.056	(12.365)	16.501	(12.015)
		0.375	ARL_{Exp}	2.368	(< 0.001)	21.686	(< 0.001)	10.050	(< 0.001)
			ARL_{NIE}	2.368	(12.952)	21.686	(12.986)	10.050	(12.226)
		0.500	ARL_{Exp}	1.388	(< 0.001)	11.732	(< 0.001)	7.036	(< 0.001)
			ARL_{NIE}	1.388	(12.235)	11.732	(12.633)	7.036	(12.468)
		0.625	ARL_{Exp}	1.133	(< 0.001)	7.121	(< 0.001)	5.361	(< 0.001)
			ARL_{NIE}	1.133	(12.653)	7.121	(12.465)	5.361	(12.546)
		0.750	ARL_{Exp}	1.053	(< 0.001)	4.762	(< 0.001)	4.326	(< 0.001)
			ARL_{NIE}	1.053	(13.012)	4.762	(12.765)	4.326	(12.755)
		0.875	ARL_{Exp}	1.024	(< 0.001)	3.456	(< 0.001)	3.639	(< 0.001)
			ARL_{NIE}	1.024	(12.985)	3.456	(13.011)	3.639	(12.653)
		1.000	ARL_{Exp}	1.012	(< 0.001)	2.684	(< 0.001)	3.157	(< 0.001)
			ARL_{NIE}	1.012	(12.563)	2.684	(12.466)	3.157	(12.864)
Coefficient parameters		δ	λ		0.05		0.10		0.30
Θ_1	ϖ_1		H		0.0000000397522		0.00168855		0.11947392
-0.3	0.1	0.125	ARL_{Exp}	29.342	(< 0.001)	108.619	(< 0.001)	26.844	(< 0.001)
			ARL_{NIE}	29.342	(12.035)	108.619	(12.465)	26.844	(12.065)
		0.250	ARL_{Exp}	13.130	(< 0.001)	40.756	(< 0.001)	11.911	(< 0.001)
			ARL_{NIE}	13.130	(12.465)	40.756	(12.597)	11.911	(13.578)
		0.375	ARL_{Exp}	7.950	(< 0.001)	18.453	(< 0.001)	7.191	(< 0.001)
			ARL_{NIE}	7.950	(12.597)	18.453	(11.975)	7.191	(12.796)
		0.500	ARL_{Exp}	5.567	(< 0.001)	9.725	(< 0.001)	5.037	(< 0.001)
			ARL_{NIE}	5.567	(12.945)	9.725	(13.154)	5.037	(11.974)
		0.625	ARL_{Exp}	4.260	(< 0.001)	5.823	(< 0.001)	3.863	(< 0.001)
			ARL_{NIE}	4.260	(12.359)	5.823	(12.562)	3.863	(11.958)
		0.750	ARL_{Exp}	3.461	(< 0.001)	3.886	(< 0.001)	3.149	(< 0.001)
			ARL_{NIE}	3.461	(12.795)	3.886	(12.015)	3.149	(13.044)
		0.875	ARL_{Exp}	2.935	(< 0.001)	2.841	(< 0.001)	2.682	(< 0.001)
			ARL_{NIE}	2.935	(12.496)	2.841	(12.226)	2.682	(12.983)
		1.000	ARL_{Exp}	2.570	(< 0.001)	2.237	(< 0.001)	2.358	(< 0.001)
			ARL_{NIE}	2.570	(11.866)	2.237	(12.468)	2.358	(12.546)

The values in parentheses are the processing times in seconds.

Table 4. ARL_1 values using the explicit formula and NIE methods for the EWMA control chart with the FISMAX(0.125, 1, 2)$_{12}$ model and exponential white noise (ARL_0 = 370)

Coefficient parameters			δ	λ	0.05		0.10		0.30	
Θ_1	ϖ_1	ϖ_2		H	0.0000000755249		0.00323183		0.24149753	
0.3	0.1	0.3	0.125	ARL_{Exp}	39.361	(< 0.001)	116.979	(< 0.001)	37.121	(< 0.001)
				ARL_{NIE}	39.361	(11.985)	116.979	(12.186)	37.121	(12.022)
			0.250	ARL_{Exp}	7.202	(< 0.001)	46.453	(< 0.001)	16.963	(< 0.001)
				ARL_{NIE}	7.202	(12.031)	46.453	(12.998)	16.963	(12.560)
			0.375	ARL_{Exp}	2.384	(< 0.001)	21.934	(< 0.001)	10.338	(< 0.001)
				ARL_{NIE}	2.384	(12.598)	21.934	(12.235)	10.338	(13.012)
			0.500	ARL_{Exp}	1.394	(< 0.001)	11.890	(< 0.001)	7.236	(< 0.001)
				ARL_{NIE}	1.394	(12.687)	11.890	(11.721)	7.236	(12.896)
			0.625	ARL_{Exp}	1.135	(< 0.001)	7.224	(< 0.001)	5.511	(< 0.001)
				ARL_{NIE}	1.135	(13.015)	7.224	(12.151)	5.511	(12.703)
			0.750	ARL_{Exp}	1.054	(< 0.001)	4.833	(< 0.001)	4.444	(< 0.001)
				ARL_{NIE}	1.054	(12.981)	4.833	(12.138)	4.444	(11.985)
			0.875	ARL_{Exp}	1.024	(< 0.001)	3.506	(< 0.001)	3.735	(< 0.001)
				ARL_{NIE}	1.024	(11.978)	3.506	(12.065)	3.735	(12.065)
			1.000	ARL_{Exp}	1.012	(< 0.001)	2.721	(< 0.001)	3.237	(< 0.001)
				ARL_{NIE}	1.012	(12.746)	2.721	(13.578)	3.237	(12.564)
Coefficient parameters			δ	λ	0.05		0.10		0.30	
Θ_1	ϖ_1	ϖ_2		H	0.0000000414489		0.001761233		0.124923602	
-0.3	0.1	0.3	0.125	ARL_{Exp}	36.887	(< 0.001)	109.143	(< 0.001)	27.331	(< 0.001)
				ARL_{NIE}	36.887	(12.462)	109.143	(13.048)	27.331	(12.872)
			0.250	ARL_{Exp}	6.501	(< 0.001)	41.103	(< 0.001)	12.147	(< 0.001)
				ARL_{NIE}	6.501	(13.015)	41.103	(12.975)	12.147	(11.897)
			0.375	ARL_{Exp}	2.175	(< 0.001)	18.660	(< 0.001)	7.338	(< 0.001)
				ARL_{NIE}	2.175	(12.356)	18.660	(12.151)	7.338	(12.035)
			0.500	ARL_{Exp}	1.322	(< 0.001)	9.851	(< 0.001)	5.140	(< 0.001)
				ARL_{NIE}	1.322	(11.956)	9.851	(12.138)	5.140	(12.465)
			0.625	ARL_{Exp}	1.107	(< 0.001)	5.904	(< 0.001)	3.940	(< 0.001)
				ARL_{NIE}	1.107	(12.687)	5.904	(12.065)	3.940	(12.597)
			0.750	ARL_{Exp}	1.041	(< 0.001)	3.940	(< 0.001)	3.210	(< 0.001)
				ARL_{NIE}	1.041	(13.015)	3.940	(13.578)	3.210	(12.952)
			0.875	ARL_{Exp}	1.018	(< 0.001)	2.878	(< 0.001)	2.731	(< 0.001)
				ARL_{NIE}	1.018	(12.981)	2.878	(12.796)	2.731	(12.235)
			1.000	ARL_{Exp}	1.009	(< 0.001)	2.264	(< 0.001)	2.399	(< 0.001)
				ARL_{NIE}	1.009	(11.978)	2.264	(11.974)	2.399	(12.667)

The values in parentheses are the processing times in seconds.

Table 5. ARL_1 values using the explicit formula and NIE methods for the EWMA control chart with the FISMAX(0.25, 1, 2)$_{12}$ model and exponential white noise (ARL_0 = 370)

Coefficient parameters			δ	λ	0.05		0.10		0.30	
Θ_1	ϖ_1	ϖ_2		H	0.000000062796		0.002680062		0.19628007	
0.3	0.1	0.3	0.125	ARL_{Exp}	38.582	(< 0.001)	114.502	(< 0.001)	33.368	(< 0.001)
				ARL_{NIE}	38.582	(12.465)	114.502	(12.945)	33.368	(12.531)
			0.250	ARL_{Exp}	6.977	(< 0.001)	44.729	(< 0.001)	15.109	(< 0.001)
				ARL_{NIE}	6.977	(12.635)	44.729	(12.359)	15.109	(12.152)
			0.375	ARL_{Exp}	2.316	(< 0.001)	20.862	(< 0.001)	9.183	(< 0.001)
				ARL_{NIE}	2.316	(12.454)	20.862	(12.795)	9.183	(12.235)
			0.500	ARL_{Exp}	1.370	(< 0.001)	11.214	(< 0.001)	6.430	(< 0.001)
				ARL_{NIE}	1.370	(12.335)	11.214	(12.496)	6.430	(12.465)
			0.625	ARL_{Exp}	1.126	(< 0.001)	6.782	(< 0.001)	4.907	(< 0.001)
				ARL_{NIE}	1.126	(12.986)	6.782	(12.667)	4.907	(12.866)
			0.750	ARL_{Exp}	1.050	(< 0.001)	4.531	(< 0.001)	3.970	(< 0.001)
				ARL_{NIE}	1.050	(12.565)	4.531	(13.048)	3.970	(13.013)
			0.875	ARL_{Exp}	1.022	(< 0.001)	3.292	(< 0.001)	3.349	(< 0.001)
				ARL_{NIE}	1.022	(12.456)	3.292	(12.975)	3.349	(12.565)
			1.000	ARL_{Exp}	1.011	(< 0.001)	2.564	(< 0.001)	2.915	(< 0.001)
				ARL_{NIE}	1.011	(12.865)	2.564	(12.115)	2.915	(12.456)
Coefficient parameters			δ	λ	0.05		0.10		0.30	
Θ_1	ϖ_1	ϖ_2		H	0.0000000344632		0.001462305		0.10268343	
-0.3	0.1	0.3	0.125	ARL_{Exp}	36.158	(< 0.001)	106.853	(< 0.001)	25.301	(< 0.001)
				ARL_{NIE}	36.158	(12.798)	106.853	(12.226)	25.301	(12.687)
			0.250	ARL_{Exp}	6.301	(< 0.001)	39.597	(< 0.001)	11.162	(< 0.001)
				ARL_{NIE}	6.301	(13.016)	39.597	(12.186)	11.162	(13.015)
			0.375	ARL_{Exp}	2.117	(< 0.001)	17.765	(< 0.001)	6.727	(< 0.001)
				ARL_{NIE}	2.117	(11.894)	17.765	(12.998)	6.727	(12.335)
			0.500	ARL_{Exp}	1.303	(< 0.001)	9.308	(< 0.001)	4.714	(< 0.001)
				ARL_{NIE}	1.303	(12.796)	9.308	(12.235)	4.714	(12.986)
			0.625	ARL_{Exp}	1.100	(< 0.001)	5.559	(< 0.001)	3.621	(< 0.001)
				ARL_{NIE}	1.100	(11.974)	5.559	(11.721)	3.621	(12.565)
			0.750	ARL_{Exp}	1.038	(< 0.001)	3.711	(< 0.001)	2.960	(< 0.001)
				ARL_{NIE}	1.038	(11.958)	3.711	(12.151)	2.960	(12.456)
			0.875	ARL_{Exp}	1.017	(< 0.001)	2.720	(< 0.001)	2.528	(< 0.001)
				ARL_{NIE}	1.017	(13.044)	2.720	(12.138)	2.528	(12.865)
			1.000	ARL_{Exp}	1.008	(< 0.001)	2.150	(< 0.001)	2.230	(< 0.001)
				ARL_{NIE}	1.008	(12.983)	2.150	(12.065)	2.230	(12.546)

The values in parentheses are the processing times in seconds.

Table 6. ARL_1 values using the explicit formula and NIE methods for the EWMA control chart with the FISMAX(0.375, 1, 2)$_{12}$ model and exponential white noise (ARL_0 = 370)

Coefficient parameters			δ	λ		0.05		0.10		0.30
Θ_1	ϖ_1	ϖ_2		H		0.0000000536598		0.00228583		0.16508801
0.3	0.1	0.3	0.125	ARL_{Exp}	37.931	(< 0.001)	112.439	(< 0.001)	30.778	(< 0.001)
				ARL_{NIE}	37.931	(12.036)	112.439	(12.365)	30.778	(12.746)
			0.250	ARL_{Exp}	6.792	(< 0.001)	43.316	(< 0.001)	13.834	(< 0.001)
				ARL_{NIE}	6.792	(12.186)	43.316	(12.486)	13.834	(13.015)
			0.375	ARL_{Exp}	2.261	(< 0.001)	19.996	(< 0.001)	8.389	(< 0.001)
				ARL_{NIE}	2.261	(12.998)	19.996	(12.766)	8.389	(12.064)
			0.500	ARL_{Exp}	1.351	(< 0.001)	10.674	(< 0.001)	5.874	(< 0.001)
				ARL_{NIE}	1.351	(12.235)	10.674	(12.663)	5.874	(12.355)
			0.625	ARL_{Exp}	1.118	(< 0.001)	6.432	(< 0.001)	4.490	(< 0.001)
				ARL_{NIE}	1.118	(11.721)	6.432	(12.651)	4.490	(11.946)
			0.750	ARL_{Exp}	1.046	(< 0.001)	4.294	(< 0.001)	3.642	(< 0.001)
				ARL_{NIE}	1.046	(12.151)	4.294	(12.064)	3.642	(12.035)
			0.875	ARL_{Exp}	1.020	(< 0.001)	3.125	(< 0.001)	3.082	(< 0.001)
				ARL_{NIE}	1.020	(12.138)	3.125	(12.355)	3.082	(12.765)
			1.000	ARL_{Exp}	1.010	(< 0.001)	2.443	(< 0.001)	2.692	(< 0.001)
				ARL_{NIE}	1.010	(12.456)	2.443	(11.946)	2.692	(12.119)
Coefficient parameters			δ	λ		0.05		0.10		0.30
Θ_1	ϖ_1	ϖ_2		H		0.0000000294491		0.001248272		0.087034695
-0.3	0.1	0.3	0.125	ARL_{Exp}	35.549	(< 0.001)	104.944	(< 0.001)	23.786	(< 0.001)
				ARL_{NIE}	35.549	(12.865)	104.944	(12.687)	23.786	(12.795)
			0.250	ARL_{Exp}	6.137	(< 0.001)	38.361	(< 0.001)	10.431	(< 0.001)
				ARL_{NIE}	6.137	(12.346)	38.361	(13.015)	10.431	(12.953)
			0.375	ARL_{Exp}	2.070	(< 0.001)	17.041	(< 0.001)	6.275	(< 0.001)
				ARL_{NIE}	2.070	(12.798)	17.041	(12.981)	6.275	(12.201)
			0.500	ARL_{Exp}	1.287	(< 0.001)	8.873	(< 0.001)	4.400	(< 0.001)
				ARL_{NIE}	1.287	(12.065	8.873	(11.978)	4.400	(12.022)
			0.625	ARL_{Exp}	1.094	(< 0.001)	5.285	(< 0.001)	3.387	(< 0.001)
				ARL_{NIE}	1.094	(13.578)	5.285	(12.746)	3.387	(12.560)
			0.750	ARL_{Exp}	1.036	(< 0.001)	3.531	(< 0.001)	2.776	(< 0.001)
				ARL_{NIE}	1.036	(12.796)	3.531	(13.015)	2.776	(13.012)
			0.875	ARL_{Exp}	1.015	(< 0.001)	2.596	(< 0.001)	2.380	(< 0.001)
				ARL_{NIE}	1.015	(12.262)	2.596	(12.843)	2.380	(12.896)
			1.000	ARL_{Exp}	1.007	(< 0.001)	2.061	(< 0.001)	2.107	(< 0.001)
				ARL_{NIE}	1.007	(12.465)	2.061	(12.065)	2.107	(12.703

The values in parentheses are the processing times in seconds.

Table 7. ATS $_1$ values using the NIE method for the EWMA control chart with the FISMAX(D, Q, X)$_{12}$ model and exponential white noise (ARL$_0$ = 370)

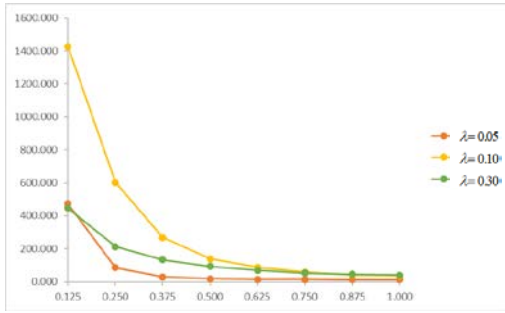
Q	X_1	X_2	δ	FISMAX(0.125, 1, X)$_{12}$			FISMAX(0.25, 1, X)$_{12}$			FISMAX(0.375, 1, X)$_{12}$		
Θ_1	ϖ_1	ϖ_2		λ =0.05	λ =0.1	λ =0.3	λ =0.05	λ =0.1	λ =0.3	λ =0.05	λ =0.1	λ =0.3
0.3	0.1		0.125	526.031	1466.085	554.817	482.855	1489.600	489.760	491.982	1460.401	432.218
			0.250	95.311	571.443	260.393	92.293	588.203	223.676	90.719	569.482	198.260
			0.375	31.655	286.577	153.968	29.750	282.621	140.929	30.670	281.614	122.871
			0.500	17.368	155.678	112.987	17.559	157.481	97.813	16.982	148.210	87.725
			0.625	13.758	99.308	83.527	14.850	95.213	76.762	14.336	88.763	67.259
			0.750	12.770	67.646	64.416	13.048	63.698	58.251	13.702	60.787	55.178
			0.875	12.527	50.282	56.539	12.255	44.034	50.573	13.297	44.966	46.044
			1.000	13.180	33.287	47.908	12.394	34.928	43.884	12.714	33.459	40.612
0.3	0.1	0.3	0.125	471.742	1425.506	446.269	480.925	1482.228	418.134	456.538	1390.308	392.296
			0.250	86.647	603.796	213.055	88.154	552.806	183.605	82.767	540.844	180.050
			0.375	30.034	268.362	134.518	28.843	266.929	112.354	29.388	255.269	101.205
			0.500	17.686	139.363	93.315	16.899	140.130	80.150	16.529	135.165	72.573
			0.625	14.772	87.779	70.006	14.622	85.908	63.133	13.104	81.371	53.638
			0.750	13.682	58.663	53.261	13.193	59.120	51.662	12.710	51.803	43.831
			0.875	12.265	42.300	45.063	12.730	42.714	42.080	12.381	38.609	39.342
			1.000	12.899	36.946	40.670	13.007	31.063	36.309	12.581	29.184	32.624
-0.3	0.1		0.125	456.398	1359.750	370.666	460.712	1422.908	359.497	353.131	1353.936	323.873
			0.250	87.195	544.558	172.145	86.084	519.483	162.771	163.665	513.403	161.728
			0.375	29.609	254.737	107.875	27.565	246.285	101.448	100.146	220.975	92.016
			0.500	17.415	129.510	77.891	17.083	132.893	70.649	72.065	127.923	60.313
			0.625	14.545	85.804	58.082	14.474	72.946	51.971	52.649	73.149	46.194
			0.750	13.351	54.708	46.746	13.201	51.146	39.983	44.283	46.690	41.076
			0.875	12.115	40.864	38.273	13.008	37.832	34.510	36.676	34.734	34.820
			1.000	12.287	29.626	35.081	13.012	28.399	31.427	30.496	27.891	29.583
-0.3	0.1	0.3	0.125	459.686	1424.098	351.805	462.750	1306.385	320.994	457.338	1331.425	304.342
			0.250	84.611	533.311	144.513	82.014	482.529	145.273	75.767	499.268	135.113
			0.375	26.874	226.738	88.313	25.180	230.909	82.978	26.492	221.209	76.561
			0.500	15.806	119.571	64.070	16.673	113.883	61.216	15.528	106.281	52.897
			0.625	14.045	71.232	49.632	13.171	65.157	45.498	14.854	67.363	42.541
			0.750	13.549	53.497	41.576	12.412	45.092	36.870	13.257	45.956	36.121
			0.875	13.215	36.827	33.414	13.266	33.015	32.523	12.446	33.340	30.692
			1.000	12.086	27.109	30.388	13.087	25.940	27.978	12.552	24.866	26.765

The explicit formula yields ATS values that approach zero across all simulated cases.

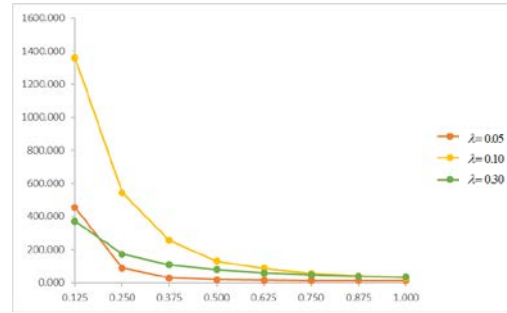
5. Application to a Real-World Scenario

The practical application of the proposed EWMA control chart is demonstrated using the dataset provided by Peerajit (2023), comprising 72 observations of the monthly value of rice exports and the Euro/Baht exchange rate from January 2012 to December 2017, while assuming that the process follows an FISMAX(0.389213, 1, 1) model with coefficients Θ_1 = 0.449405 and ϖ_1 =34366383. The white noise was assumed to follow an exponential distribution, which was verified using the Kolmogorov–Smirnov test, with a mean (β_0) of 132,271,702.9518. The process was assumed to be OOC when a shift in the process mean was within the constraint $\left(\beta_1 = \beta_0(1+\delta)\right)$. The dataset and summary of the ARL computations using both the proposed formula and the NIE methods for the proposed EWMA for $\lambda = 0.05,\ 0.1,\ 0.3$ are reported in Table 8. These parameter values were chosen so that the resulting control chart yielded ARL values close to the nominal IC ARL of 370. It can be observed from the analysis of the ARL$_1$ values that there exists a clear relationship between the magnitude of the process mean shift and the detection performance. Specifically, as the magnitude of

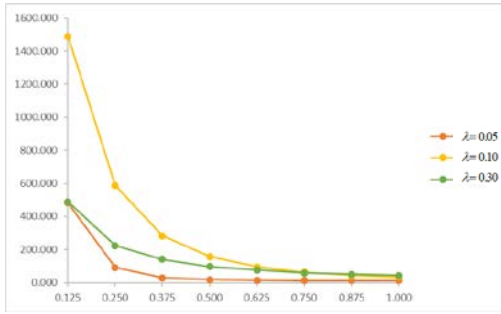
the mean shift was increased, the ARL_1 values decreased, implying faster detection of a shift in the process mean. This reduction is particularly notable when the process mean shift magnitude was less than 0.125, corresponding to small process mean changes reported in Tables 1-6. These results emphasize the sensitivity and effectiveness of the proposed EWMA control chart evaluated using the proposed formula method and are consistent with the findings provided in Tables 1-6. For moderate mean shifts, specifically when $\delta \leq 0.125$, the decrease in ARL values became less pronounced, thereby suggesting a diminishing rate of improvement in detection speed.



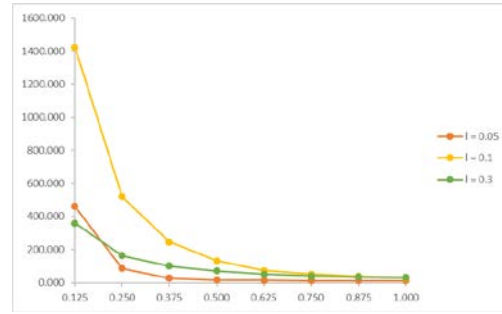
(a) FISMAX(0.125, 1, 1)$_{12}$ with $\Theta_1 = 0.3$



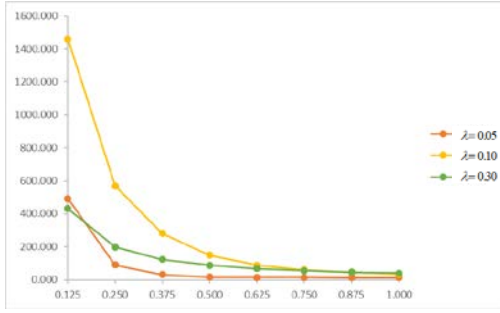
(b) FISMAX(0.125, 1, 1)$_{12}$ with $\Theta_1 = -0.3$



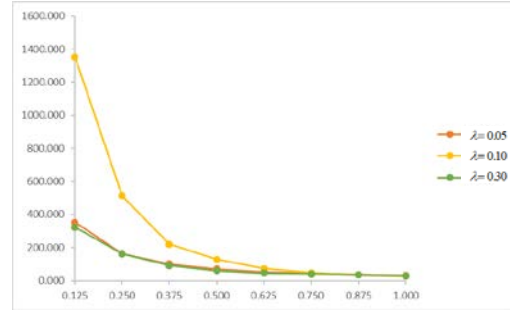
(c) FISMAX(0.250, 1, 1)$_{12}$ with $\Theta_1 = 0.3$



(d) FISMAX(0.250, 1, 1)$_{12}$ with $\Theta_1 = -0.3$



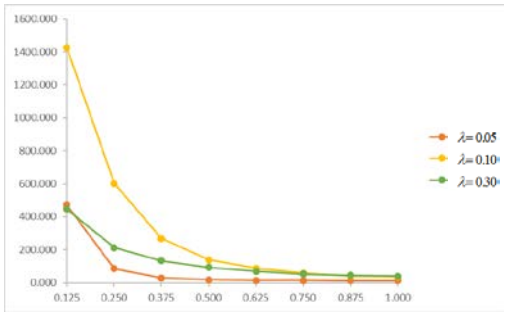
(e) FISMAX(0.375, 1, 1)$_{12}$ with $\Theta_1 = 0.3$



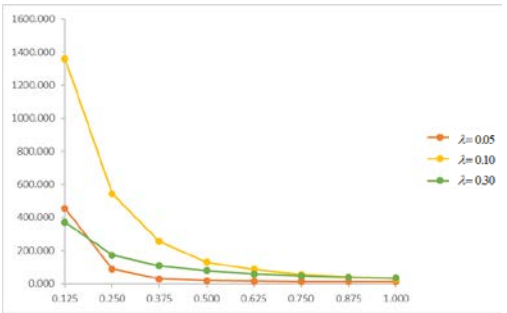
(f) FISMAX(0.375, 1, 1)$_{12}$ with $\Theta_1 = -0.3$

Figure 1. ATS comparison for different process mean shift magnitudes using the NIE method with three λ values for the FISMAX(D, 1, 1)$_{12}$, process on the EWMA control chart, showing the effect of shift size and λ on detection speed

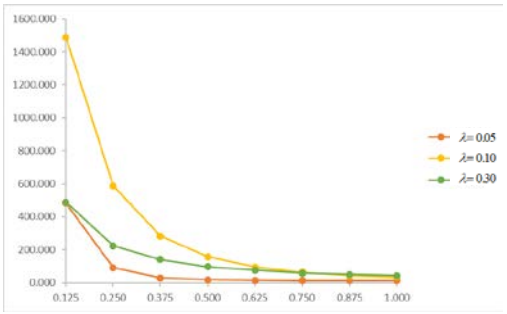
The detection performance of the proposed method in transitioning from the IC to the OOC state was evaluated based on the processing time and ATS values. It is evident that the proposed formula method is a time-independent approach that provides a more appropriate and efficient measure of control chart performance compared with the NIE method, which exhibits considerably higher ATS values than the proposed formula method.



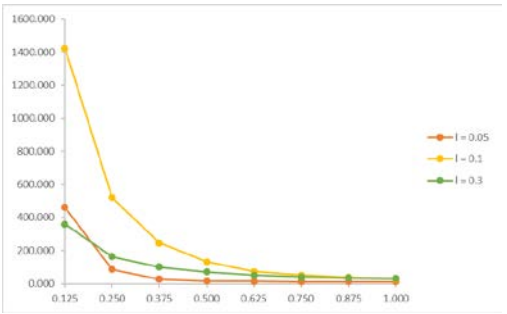
(a) FISMAX(0.125, 1, 2)$_{12}$ with Θ_1 = 0.3



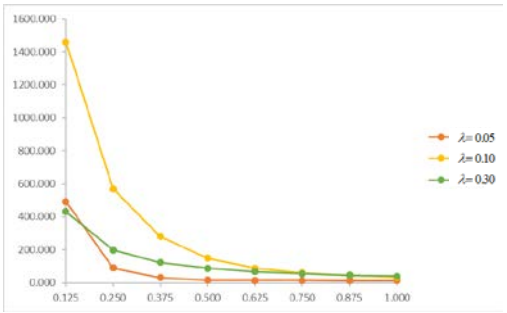
(b) FISMAX(0.125, 1, 2)$_{12}$ with Θ_1 = - 0.3



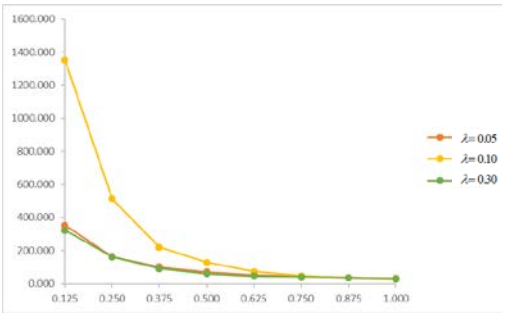
(c) FISMAX(0.250, 1, 2)$_{12}$ with Θ_1 = 0.3



(d) FISMAX(0.250, 1, 2)$_{12}$ with Θ_1 = - 0.3



(e) FISMAX(0.375, 1, 2)$_{12}$ with Θ_1 = 0.3



(f) FISMAX(0.375, 1, 2)$_{12}$ with Θ_1 = - 0.3

Figure 2. ATS comparison for different process mean shift magnitudes using the NIE method with three λ values for the FISMAX(D, 1,2)$_{12}$.process on the EWMA control chart, showing the effect of shift size and λ on detection speed

Table 8. ARL_1 and ATS values using the proposed formula and NIE methods for the EWMA control chart with the FISMAX(0.389213, 1, 1)$_{12}$ model and exponential white noise (ARL_0 = 370)

	λ = 0.05, H = 5,191,149.89				λ = 0.10, H =10,594,550				λ = 0.3, H = 34,724,431			
δ	ARL_{Exp}	ATS_{Exp}	ARL_{NIE}	ATS_{NIE}	ARL_{Exp}	ATS_{Exp}	ARL_{NIE}	ATS_{NIE}	ARL_{Exp}	ATS_{Exp}	ARL_{NIE}	ATS_{NIE}
0.125	5.646 (<0.001)	0.057	5.646 (50.654)	285.993	5.780 (<0.001)	0.058	5.780 (35.499)	205.184	6.405 (<0.001)	0.064	6.405 (12.811)	82.054
0.250	3.402 (<0.001)	0.034	3.402 (53.716)	182.742	3.469 (<0.001)	0.035	3.469 (38.311)	132.901	3.783 (<0.001)	0.038	3.783 (15.576)	58.924
0.375	2.641 (<0.001)	0.026	2.641 (56.529)	149.293	2.686 (<0.001)	0.027	2.686 (41.186)	110.626	2.895 (<0.001)	0.029	2.895 (18.42)	53.326
0.500	2.256 (<0.001)	0.023	2.256 (59.451)	134.122	2.289 (<0.001)	0.023	2.289 (43.936)	100.570	2.446 (<0.001)	0.024	2.446 (21.295)	52.088
0.625	2.022 (<0.001)	0.020	2.022 (62.326)	126.023	2.048 (<0.001)	0.020	2.048 (46.733)	95.709	2.173 (<0.001)	0.022	2.173 (24.155)	52.489
0.750	1.864 (<0.001)	0.019	1.864 (65.154)	121.4471	1.886 (<0.001)	0.019	1.886 (49.467)	93.295	1.990 (<0.001)	0.020	1.990 (27.061)	53.851
0.875	1.749 (<0.001)	0.018	1.749 (68.107)	119.119	1.768 (<0.001)	0.018	1.768 (52.279)	92.429	1.857 (<0.001)	0.019	1.857 (29.811)	55.359
1.000	1.663 (<0.001)	0.017	1.663 (70.967)	118.018	1.680 (<0.001)	0.017	1.680 (55.029)	92.449	1.757 (<0.001)	0.018	1.757 (32.686)	57.429

6. Conclusions and Recommendations

We proposed an explicit formula method for deriving the ARL for the EWMA control chart with a long-memory FISMAX process and exponential white noise. The accuracy of the proposed formula method was validated against an NIE method constructed using the composite midpoint rule; they demonstrated strong agreement across all process mean shift magnitudes and long-memory conditions. The analysis revealed that as the process mean shift increased, the ARL_1 value decreased, thereby indicating faster detection performance. This effect was most pronounced for small shifts ($\delta < 0.125$), which is consistent with previous findings (Peerajit 2025), while ARL_1 values remained stable for moderate and large shifts. In terms of computational performance, the proposed method required only a fraction of a second to compute, compared with 11-13 seconds for the NIE method. Moreover, ATS results confirmed that $\lambda = 0.05$ yielded the most effective detection across all conditions. Overall, the proposed formula-based method is an accurate and computationally efficient alternative for ARL computation and ATS evaluation for a FISMAX process with exponential white noise on the EWMA control chart, thereby highlighting its strong potential for practical process monitoring and quality improvement applications.

The findings of this study provide meaningful insights for practitioners and researchers in the field of SPC. The proposed formula-based method offers a computationally efficient and accurate tool for monitoring process performance in real-time applications, particularly when dealing with large-scale or memory-dependent data. Its ultra-fast computation time enables quick adaptation to changing process conditions, thus making it highly suitable for use in automated production environments, online quality control systems, and predictive maintenance frameworks. In addition, the demonstrated robustness of the method under both short- and long-memory conditions enhances its applicability across diverse industrial settings, including manufacturing.

In future research, the proposed formula-based approach will be extended to more complex process monitoring frameworks, such as the multivariate or adaptive EWMA control chart. Further exploration into integrating this method with machine learning algorithms could enhance its predictive capabilities for early fault detection and dynamic process adjustment. Comparative studies involving other benchmark methods may also help refine parameter optimization and expand its use in high-dimensional and non-stationary process environments.

Acknowledgements

The author gratefully acknowledges the editor and referees for their valuable comments and suggestions which greatly improve this paper. This research was funded by King Mongkut's University of Technology North Bangkok, Contract no. KMUTNB-68-BASIC-12.

References

Areepong Y, Sukparungsee S. An integral equation approach to EWMA chart for detecting a change in lognormal distribution. Thail Stat. 2010; 8: 47-61.

Areepong Y, Peerajit W. Integral equation solutions for the average run length for monitoring shifts in the mean of a generalized seasonal ARFIMAX$(P, D, Q, r)_s$ process running on a CUSUM control chart. PLoS ONE. 2022; 17(2), e0264283.

Atienza OO, Tang LC and Ang BW. A CUSUM scheme for autocorrelated observations. J Qual Technol. 2002; 34(2): 187-199.

Barbara PO, et al. Invariance of the first difference in ARFIMA models. Comput Stat. 2006; 21: 445-461.

Bagshaw M, Johnson RA. The effect of serial correlation on the performance of CUSUM tests. Technometrics. 1975; 16(1): 103-112.

Böhm, W., Hackl, P. The effect of serial correlation on the in-control average run length of cumulative score charts. J. Stat. Plan. Inference.1996; 54(1): 15–30.

Champ CW, Rigdon SE. A comparison of the Markov chain and the integral equation approaches for evaluating the run length distribution of quality control charts. Commun Stat Simul Comput. 1991; 20: 191-204.

Chang YM, Wu TL. On average run lengths of control charts for autocorrelated processes. Methodol Comput Appl Prob. 2011; 13, 419-431.

Charles ST, Reynolds CA, Gatz M. Age-related differences and change in positive and negative affect over 23 years. J Pers Soc Psychol. 2001; 80(1), 136-151.

Crowder SV. A Simple method for studying run length distributions of exponentially weighted moving average charts. Technometrics. 1987; 29: 401-407.

Degiannakis, S. ARFIMAX and ARFIMAX-TARCH realized volatility modeling. J Appl Stat. 2008; 35(10), 1169-1180.

Ebens H. Realized stock index volatility. Working Paper No. 420, Department of Economics, Johns Hopkins University; 1999.

Granger CWJ, Joyeux R. An introduction to long memory time series models and fractional differencing. J Time Ser Anal. 1980; 1(1): 15-29.

Hawkins DM, Olwell DH. Cumulative Sum Charts and Charting for Quality Improvement. New York: Springer; 1998.

He D, Grigoryan A. Multivariate multiple sampling charts. IIE Transactions. 2005; 37: 509-521.

Hosking JRM. Fractional differencing. Biometrika. 1981; 68(1): 165-176.

Jacob PA, Lewis PAW. A mixed autoregressive-moving average exponential sequence and point process (EARMA 1,1). Adv Appl Prob. 1977; 9(1): 87-104.

Jin M, Tsung F. A chart allocation strategy for multistage processes. IIE Transactions. 2009; 41: 790-803.

Johnson RA, Bagshaw M. The effect of serial correlation on the performance of CUSUM tests. Technometrics. 1974; 16(1): 103-112.

Knoth S, Frisén M. Minimax optimality of CUSUM for an autoregressive model. Stat Neerl. 2012; 66 (4): 357-379.

Lu, CW, Reynolds MR. CUSUM charts for monitoring an autocorrelated process. J Qual Technol. 2001; 33(3), 316-334.

Montgomery DC. Introduction to Statistical Quality Control. 6th ed. New York: John Wiley & Sons; 2009.

Mohamed I, Hocine F. Bayesian estimation of an AR(1) process with exponential white noise. J Theor Appl Stat. 2003; 37(5): 365-372.

Mostafaei H, Sakhabakhsh L. Using SARFIMA model to study and predict Iran's oil supply. Int J Energy Econ Policy. 2012; 2(1): 41-49.

Nikiforov IV. Sequential analysis applied to autoregressive processes. Autom Remote Control. 1975; 36: 1365-1368.

Ndongo M, et al. Estimation of long-memory parameters for seasonal fractional ARIMA with stable innovations. Stat Methodol. 2010; 7: 141-151.

Page ES. Continuous inspection schemes. Biometrika. 1954; 41(1-2): 100-115.

Pan JN, Chen ST. Monitoring long-memory air quality data using ARFIMA model. Environmetrics. 2008; 19: 209-219.

Peerajit W. Cumulative sum control chart applied to monitor shifts in the mean of a long-memory ARFIMAX(p, d^*, q, r) process with exponential white noise. Thail Stat. 2022; 20(1): 144-161.

Peerajit W. Developing average run length for monitoring changes in the mean in the presence of long memory under seasonal fractionally integrated MAX model. Math Stat. 2023; 2(1): 34-50.

Peerajit, W. Optimizing the EWMA control chart to detect changes in the mean of a long-memory seasonal fractionally integrated moving average and an exogenous variable process with exponential white noise and its application to electrical output data. WSEAS Transactions on Systems and Control. 2025; 20: 25-41.

Pereira IMS, Turkrman MA. Bayesian prediction in threshold autoregressive models with exponential white noise. Sociedad de Estadisticae Investigacion Operativa Test. 2004; 13(1): 45-64.

Piyaphon P, Areepong Y, Sukparungsee S. Exact expression of average run length of EWMA chart for SARIMA(P, D, Q)$_L$ procedure. Int J Appl Math Stat. 2014; 52: 62-73.

Rabyk L, Schmid W. EWMA control charts for detecting changes in the mean of a long-memory process. Metrika. 2016; 79(3): 267-301.

Reisen VA, et al. A semiparametric approach to estimate two seasonal fractional parameters in the SARFIMA model. Math Comput Simul. 2014; 98: 1-17.

Ramjee R. Quality control charts and persistent processes. PhD [dissertation]. Stevens Institute of Technology; 2000.

Ramjee R, Crato N, Ray BK. A note on moving average forecasts of long memory processes with an application to quality control. Int J Forecasting. 2002; 18(2): 291-297.

Roberts SW. Control chart tests based on geometric moving average. Technometrics. 1959; 1(3): 239-250.

Shewhart WA. Economic control of quality of manufacturing product. New York: Van Nostrand; 1931.

Shamsuzzaman M, Lam YC, Wu Z. Control chart system with independent quality characteristics. Int J Adv Manuf Technol. 2005; 26: 1298–1305.

Sunthornwat R, Areepong Y. Average run length on CUSUM control chart for seasonal and non-seasonal moving average processes with exogenous variables. Symmetry. 2020; 12(1): 1-15.

Suparman S. A new estimation procedure using a reversible jump MCMC algorithm for AR models of exponential white noise. Int J GEOMATE. 2018; 15(49): 85-91.

Yashchin E. Performance of CUSUM control schemes for serially correlated observations. Technometrics. 1993; 35: 37-52.

Zou C, Tsung F, Liu Y. A change point approach for phase I analysis in multistage processes. Technometrics, 2008; 50: 344-356.

Zhang S, Wu Z. Monitoring the process mean and variance using a weighted loss function CUSUM scheme with variable sampling intervals. IIE Transactions, 2006; 38: 377-387.